Oxyntomodulin regulates resetting of the liver circadian clock by food

Dominic Landgraf, Anthony H Tsang, Alexei Leliavski, Christiane E Koch, Johanna L Barclay, Daniel J Drucker, Henrik Oster

DOI: http://dx.doi.org/10.7554/eLife.06253

Cite as: eLife 2015;10.7554/eLife.06253

Received: 23 December 2014
Accepted: 27 March 2015
Published: 30 March 2015

Title: Oxyntomodulin regulates resetting of the liver circadian clock by food

Authors: Dominic Landgraf[1,2,5], Anthony H. Tsang[1,2,3], Alexei Leliavski[2,3], Christiane E. Koch[3], Johanna L. Barclay[2], Daniel J. Drucker[4], and Henrik Oster[2,3,*]

[1] Contributed equally

[2] Circadian Rhythms Group, Max Planck Institute for Biophysical Chemistry, Göttingen, Germany.

[3] Chronophysiology Group, Medical Department I, University of Lübeck, Lübeck, Germany.

[4] Department of Medicine, Lunenfeld-Tanenbaum Research Institute, Mount Sinai Hospital, University of Toronto, Toronto, Ontario, Canada.

[5] Current address: Department of Psychiatry and Center for Chronobiology, University of California San Diego, La Jolla, California, United States of America.

* Correspondence to: henrik.oster@uksh.de

Running title: Oxyntomodulin and liver clock resetting

Keywords: circadian clock, food resetting, liver, oxyntomodulin, *Per* induction

Abstract:

Circadian clocks coordinate 24-hr rhythms of behavior and physiology. In mammals, a master clock residing in the suprachiasmatic nucleus (SCN) is reset by the light-dark cycle, while timed food intake is a potent synchronizer of peripheral clocks such as the liver. Alterations in food intake rhythms can uncouple peripheral clocks from the SCN, resulting in internal desynchrony, which promotes obesity and metabolic disorders. Pancreas-derived hormones such as insulin and glucagon have been implicated in signaling mealtime to peripheral clocks. Here we identify a novel, more direct pathway of food-driven liver clock resetting involving oxyntomodulin (OXM). In mice, food intake stimulates OXM secretion from the gut, which resets liver transcription rhythms via induction of the core clock genes *Per1* and *2*. Inhibition of OXM signaling blocks food-mediated resetting of hepatocyte clocks. These data reveal a direct link between gastric filling with food and circadian rhythm phasing in metabolic tissues.

Introduction:

Extended night or rotating shift work is associated with an elevated risk for developing cancer, cardiovascular disease, immune deficiency, mood disorders, and metabolic alterations (1, 2). One major factor believed to contribute to this adverse health impact of shift work is a disruption of endogenous circadian clocks by mistimed resetting stimuli, so called *Zeitgebers*, as a consequence of altered sleep/wake schedules. Most organisms have evolved internal timekeepers to anticipate the environmental changes brought about by the Earth's rotation around its axis. In mammals, these so called circadian clocks are based on ubiquitously expressed cellular interlocking transcriptional-translational feedback loops (TTLs) of clock genes/proteins (3). In the core TTL, the transcriptional activators circadian locomotor output cycles kaput (CLOCK) and brain and muscle ARNT-like 1 (BMAL1; ARNTL) regulate the expression of two *Cryptochrome* (*Cry1/2*) and three *Period* (*Per1-3*) genes. Towards the end of the day, PER and CRY proteins translocate into the nucleus where they inhibit their own abundance via inhibition of CLOCK/BMAL1. Further accessory loops serve to stabilize this 24-hr feedback rhythm and integrate the clock with cellular processes (4). The clock machinery regulates physiology via orchestration of tissue-specific rhythmic expression of clock output genes (5).

The external light-dark cycle is the most prominent *Zeitgeber* of the central circadian pacemaker located in the suprachiasmatic nucleus (SCN) of the hypothalamus (6). The SCN receives light information from the retina and synchronizes peripheral clocks throughout the body via neuronal and hormonal pathways (7). While the SCN itself is largely non-responsive to non-photic timing signals such as food intake, meal timing is an important *Zeitgeber* for clocks in peripheral tissues (8). If food access is restricted to the normal rest phase of an organism, i.e. the night for humans or daytime for nocturnal rodents, peripheral clocks become uncoupled from the SCN and adapt to the timing of food availability (9). Shift workers often eat at times when their digestive timing system is poorly prepared for food (10). Animal studies suggest that food intake during the

normal rest phase promotes obesity (11, 12) and peripheral circadian uncoupling has been suggested to contribute to the development of metabolic disorders in night shift workers (13, 14). Various other factors can regulate clock gene expression in peripheral tissues, including glucocorticoids and changes in body temperature or autonomic signaling (7). The mechanisms of food-dependent peripheral clock resetting, however, remain poorly understood. Metabolic hormones such as insulin, ghrelin and glucagon have been shown to affect circadian rhythms associated with food restriction (15-18). While ghrelin appears to act primarily on the brain, insulin and glucagon levels are mainly regulated via blood glucose. However, it was shown that carbohydrate intake alone has only a minor phase resetting capacity, while complex foods show much stronger effects (19), indicating that other factors must be involved. Besides the pancreas, other organs – notably including the gastrointestinal tract itself – show acute hormonal responses to fasting or feeding (20). This led us to hypothesize that postprandial, gut-derived signals may be implicated in food-driven resetting of peripheral clocks. In a screen using rhythmic liver slice cultures, we identified oxyntomodulin (OXM) as a potent resetting signal of liver circadian clocks. OXM is an anorexigenic incretin hormone produced in the gut by prohormone convertase 1/3-driven cleavage of the precursor preproglucagon (for review see (21)). It modulates energy and glucose metabolism by acting on various tissues, including brain, liver, and pancreas (22, 23). Since OXM secretion is dependent on food intake we hypothesized that OXM may directly link food intake to hepatic transcriptional activity by resetting of the liver clock.

Results:

OXM resets the circadian clock in organotypic liver slice cultures

We screened a commercially available metabolic peptide library (Obesity Peptide Library, Phoenix Europe GmbH; DE) for factors capable of resetting luciferase activity rhythms in organotypic liver slice cultures from *Per2::LUC* circadian reporter mice (24). Interestingly, out of 200 peptides applied during the descending phase (~180°, corresponding to the early morning) of the luciferase activity rhythm, only a few produced marked phase shifts, including three proglucagon-derived peptide (PGDP) hormones: exendin-4, OXM and glucagon (GCG) (Fig. 1 – source data 1). Exendin-4 has been isolated from the salivary gland of the *Gila* monster, with no analogue in rodents or humans. To compare the effectiveness of mammalian PGDPs in liver clock resetting, we treated slices with increasing doses of OXM, GCG, and the three other commercially available PGDPs, glicentin-related pancreatic polypeptide (GRPP), glucagon-like peptide-1 (GLP-1), and glucagon-like peptide-2 (GLP-2) (Fig. 1A). GLP-1, GLP-2, and GRPP (0.5-450 nM) had no significant resetting effects on PER2::LUC phase compared to PBS-treatment (Fig. 1B-D). GCG resulted in phase delays of up to 3 h, but only at relatively high concentrations (Fig. 1E). In contrast, OXM reset PER2::LUC rhythms in liver slices at much lower doses, resulting in phase delays of up to 8 h at higher concentrations (Fig. 1F). To act as a true *Zeitgeber* signal one would expect differential OXM effects depending on treatment time, i.e. a circadian *gating* effect. We tested this by applying OXM at different phases of the PER2::LUC rhythm. To validate the setup, slices were treated at different PER2::LUC phases with 100 µM of the glucocorticoid analog dexamethasone (DEX), which was previously shown to reset hepatocyte clocks *in vivo* (25). In a phase-dependent manner DEX treatment reset PER2::LUC activity rhythms in slices (Fig. 1 – fig. suppl. 1). Very similar to what had been observed after DEX treatment in animals (25), application in the first quarter of the PER2::LUC activity rhythm (0-90°) resulted in phase delays, while later treatments produced phase advances (100-180°) or had no marked effect (around 270°). Likewise, OXM effects were phase-dependent. Delays were

predominantly observed at 90-210° of the PER2::LUC cycle with a maximum around 180°, while only modest phase shifts were seen at 270-360° (Fig. 1G). Though GCG also showed potential in resetting liver clock rhythms, OXM emerged as the most potent liver clock synchronizer from our screen. Moreover, contrary to glucagon, OXM secretion is directly induced by food consumption in humans (26), making it an attractive candidate for linking meal timing and clock function. Therefore we focused on OXM for further analyses.

OXM signals via the glucagon receptor to activate *Per* gene expression in liver slices

So far no OXM-specific receptor has been identified, however OXM can bind to and activate both glucagon (GCGR) and GLP-1 receptors (GLPR) (27). *Gcgr* transcripts are strongly expressed in the murine liver (28). In contrast, the majority of previous studies failed to detect a full-length *Glp1r* mRNA in murine hepatocytes (29-31). We performed RT-PCR analyses for all annotated coding *Glp1r* exons on cDNA preparations from wild-type mouse livers with pancreas as positive control. *Glp1r* transcripts were present in pancreas, but undetectable in liver samples (Fig. 2 – fig. suppl. 1), in line with the absence of significant liver clock resetting effects of GLP-1 (Fig. 1B) and potent resetting of PER2::LUC rhythms by OXM treatment in slices from *PER2::LUC x Glp1r*$^{-/-}$ mice (Fig. 2A). On the other hand, blocking GCGR signaling by co-treatment with 2-(4-Pyridyl)-5-(4-chlorophenyl)-3-(5-bromo-2-propyloxyphenyl)pyrrol (Calbiochem Glucagon Receptor Inhibitor II; GRI-2) potently inhibited GCG- and OXM-induced clock resetting in *Per2::LUC* slices (Fig. 2B).

GCGR is a G protein-coupled receptor that, via protein kinase A, leads to phosphorylation and activation of the transcription factor cyclic adenosine monophosphate (cAMP) response element-binding protein (CREB) (32, 33). This pathway is reminiscent of the SCN, where nocturnal light exposure induces *Per* gene transcription via cAMP signaling and CREB activation downstream of the N-methyl-D-aspartate (NMDA) receptor (34). To investigate if OXM would impinge on

the hepatic clock machinery in a similar way we treated liver explants with OXM and performed chromatin immunoprecipitation (ChIP) analysis to measure CREB binding to cAMP response elements (*CRE*) in the *Per1* gene promoter. 30 min after OXM treatment, CREB binding was significantly increased at the *Per1* CRE, but not at downstream sequences (Fig. 2C). In addition, we analyzed clock gene expression in liver slices at different intervals after treatment with OXM at 180°. *Per1* expression was transiently induced 60 min after addition of OXM to the medium, returning back to normal levels after 120 min (Fig. 3A). Similarly, *Per2* was induced by OXM after 60 min, but mRNA levels remained high even after 120 min (Fig. 3B). No significant effect was seen on *Bmal1* expression at all time points (Fig. 3C). In line with the absence of OXM-induced phase shifts at 360° (Fig. 1G), *Per1/2* and *Bmal1* mRNA levels were unaffected by OXM treatment at this phase (Fig. 3D-F). Induction of *Per1* and *Per2* expression was preserved in *Glp1r*$^{-/-}$ slices, suggesting that hepatic OXM effects are independent of GLP-1R signaling (Fig. 3G, H).

OXM resets the liver clock *in vivo*

To test if the effect of OXM on liver clock gene activity is preserved *in vivo*, we analyzed hepatic *Per1/2* transcription after OXM treatment in wild-type mice. Analogous to what we observed in slices, robust *Per1* and *Per2* induction was observed after *i.v.* injection of OXM at *Zeitgeber* time (ZT) 3 (Fig. 4A). When animals were treated with OXM at the opposite phase of the LD cycle (ZT15) - a time when nocturnal mice usually eat and, thus, no food-mediated clock shifts would be expected - no induction of *Per* gene expression was observed (Fig. 4B). Of note, *in situ* hybridization showed no acute effect of OXM treatment on *Per* expression in the SCN at ZT3 (Fig. 4C), indicating that OXM acts primarily on the liver clock and in line with the observed phase stability of the SCN clock under time-restricted feeding (RF) conditions (9).

To assess OXM effects on liver clock phase, we next treated wild-type mice with either PBS or OXM at the beginning of their rest phase on the first day in constant darkness (DD) and under fasting conditions, thus excluding potential confounding effects of light exposure or food intake. *Per2* and *Dbp* expression were determined from liver cDNA preparations at different time points using qPCR. We detected phase delays of *Per2* and *Dbp* mRNA rhythms in livers of OXM-treated mice relative to those in PBS-injected control animals (Fig. 4D), in line with the phase-delaying effects of OXM administration in slices at this time (Fig. 1G). In addition, *Per2,* but not *Dbp,* rhythms appeared dampened after OXM injection.

Tissue clocks regulate local physiology via coordination of transcriptional programs. To test if OXM treatment would impinge on hepatic energy metabolism, we analyzed the expression of important metabolic transcripts after OXM treatment. Similar to what we observed for clock gene activity, transcript profiles of genes involved in liver carbohydrate metabolism were found either phase delayed (*Foxo1* and *Pdk4*; Fig. 5A, B) and/or dampened (*Foxo1* and *Pklr*; Fig. 5A, C). Of note *Pepck*, which was previously described as a clock output gene in liver (35) was not rhythmic under these conditions and OXM had no further effect on *Pepck* mRNA levels (Fig. 5D). Expression levels of the glucose transporter *Slc2a2* (*Glut2*) and the pyruvate transporter *Slc16a7* were also dampened or phase-delayed, respectively (Fig. 5E, F).

In summary, our data so far show that OXM treatment resets liver circadian mRNA rhythms in a phase- and dose-dependent manner, indicating that it may be involved in food-induced resetting of the liver circadian clock and metabolic machinery.

Food intake-mediated OXM induction and liver clock resetting

In humans, OXM levels in the blood rise in response to food intake (26). To test whether this effect is conserved in mice, we determined diurnal plasma oxyntomodulin-like immunoreactivity

(OLI) profiles in mice with *ad libitum* food access and in fasted animals. In fed mice OLI levels were elevated during the active dark phase, while under fasting conditions OLI concentrations were constant and consistently low (Fig. 6A). In line with this, non-rhythmic *Gcg* mRNA expression in the gut was observed under fasting conditions (data not shown). These data suggest a link between food intake and OXM secretion. To test this more directly we used a 12-h fasting-refeeding paradigm. Mean fasting OLI levels in the early morning (ZT1) were ~3.5 ng/ml, but showed high inter-individual variation (Fig. 6B). Upon food intake, a rapid increase (relative to individual fasting levels) was observed after 20 min. This effect persisted for more than 1 h before returning to baseline levels (Fig. 6C). Of note, OLI induction after OXM injections were about 2-3fold higher than what was observed after refeeding (Fig. 6 – figure supplement 1). To test if postprandial OLI induction is sufficient to affect liver clock gene expression, we analyzed *Per1/2* mRNA levels in livers of wild-type mice after fasting-refeeding. Parallel to the rise in plasma OLI, we observed a transient postprandial increase of hepatic *Per1* expression. *Per2* expression showed a delayed, but more persistent induction (Fig. 6D). Food-mediated *Per* activation was partly inhibited by treatment with purified *anti*-OXM IgG to neutralize the effects of endogenous OXM in wild-type (Fig. 6E) and in *Glp1r*$^{-/-}$ mice (Fig. 6F). Importantly, the effects of refeeding on insulin, GLP-1, and glucagon plasma levels were not affected by treatment with *anti*-OXM IgG, suggesting that these peptides are not involved in the activation of food-induced hepatic *Per* expression (Fig. 6G-I).

We next tested if OXM signaling regulates food-mediated phase resetting of the liver clock using *Per2::LUC* slice preparations. *Per2::LUC* mice were starved overnight (ZT12-24/0) and treated with either IgG or *anti*-OXM antibodies prior to re-feeding or extended starving. Animals were sacrificed at ZT4 and liver slices were prepared to determine luciferase rhythm phases. After a 12-h fast, food intake caused a significant phase delay of PER2::LUC activity in liver slices and

this effect was attenuated by OXM neutralization (Fig. 6J, K). No effect on PER2::LUC phase was seen after *anti*-OXM treatment alone (Fig. 6K).

Together, these data suggest that elevated OXM levels in response to food intake affect hepatic clock gene expression. Neutralization of endogenous OXM signaling inhibits food-induced clock gene induction and rhythm shifts, suggesting that OXM may act as a metabolic synchronizer of hepatic clocks.

Discussion:

Food intake resets circadian clocks in peripheral tissues. In consequence, eating during the normal rest phase leads to a state of internal circadian desynchrony which has been suggested to underlie metabolic deregulation under shiftwork conditions (13, 36, 37). Different mechanisms of food-related circadian synchronization have been proposed, including blood glucose-responsive peptide hormones (7, 15, 16, 18). However, food entrainment does not exclusively depend on glucose (19) and the molecular mechanisms underlying food entrainment of peripheral tissues remain poorly characterized (7). Here we identified the incretin peptide OXM as a potential direct link between food intake in the gut and resetting of hepatic clock and metabolic gene transcription.

Using an organotypic slice culture system we found that OXM – and, as was shown recently, GCG (18) – treatment can reset PER2::LUC circadian reporter activity rhythm in a dose- and phase-dependent manner (Fig. 1). Consistently, peripheral OXM injections in mice reset clock gene rhythms, as well as genes involved in hepatic carbohydrate regulation, thus impinging on hepatic energy metabolism (Figs. 4, 5). In contrast, no significant effect of OXM treatment was observed at the level of the SCN pacemaker (Fig. 4). In mice, food intake during day (i.e. the normal rest time) uncouples the liver clock from that in the SCN (35), leading to a state of internal circadian desynchrony that is associated with elevated body weight and other metabolic impairments (11, 12). In the liver, around 10 % of the transcriptome is under circadian regulation including many genes involved in energy metabolism (38, 39). Genetic ablation of the liver clock abolishes the circadian rhythms of several glucose regulatory genes and results in a perturbed diurnal profile of blood glucose (35, 40).

Our experiments suggest that OXM signaling involves activation of GCGR (Fig. 2). This is puzzling given that OXM displays a much greater capacity for clock gene induction in liver slices

than GCG itself, despite having a lower binding affinity for GCGR (17). While we cannot conclusively answer this question at the moment, there are two scenarios that might explain our observations. First, GCGR may not be the only receptor involved in OXM-mediated clock resetting. While our data suggest that GLP1R does not play a role in this context (Fig. 2, 3), an additional OXM receptor has been suggested (18, 22), the activation of which may interact with GCGR downstream signaling. Second, an additional signal may be involved that acts synergistically with OXM to activate hepatic *Per* transcription. One such candidate could be insulin, which is similarly elevated after food intake and has previously been suggested to affect liver clock rhythms (16, 18, 41). In response to food intake OXM levels go up, while GCG plasma concentrations are reduced (Fig. 6), suggesting that postprandial GCGR activation does not depend on GCG itself. Interestingly, GCG/GCGR signaling has recently been implicated in the regulation of hepatic *Bmal1* expression in response to prolonged starvation (18). Sun *et al.* show that fasting-induced GCG signaling activates *Bmal1* transcription via CREB/CRTC2 during the night. As we did not observe any acute effects of OXM treatment on *Bmal1* transcription (Fig. 3), these data suggest that GCGR signaling may have different clock targets depending on the time of activation. GCGR activation is known to induce protein kinase A-mediated nuclear translocation and DNA-binding of phosphorylated CREB on target genes (32, 33). In line with this, we show OXM-induced binding of CREB to *Per1* promoter *CRE* motifs and induction of *Per* clock gene expression (Figs. 2-4). Similar phase-dependencies were observed for *Per* induction as were seen for clock shifting (compare Figs. 1, 3, 4). For various tissues - including the SCN - it has been shown that resetting of the circadian clock involves acute up-regulation of *Per1* and *Per2* (42, 43). *Per* induction was observed after dexamethasone treatment or serum shock in fibroblast and hepatoma cells (25, 44). Light pulses given during the dark phase induce CREB activation and *Per* expression in the SCN (45, 46). In line with this, we showed *Per1* and *Per2* induction after OXM treatment. Of note, *Per* induction in liver slices was weaker than *in vivo*, suggesting that additional mechanisms may amplify OXM effects in intact animals. Along

the same line, OXM-mediated *Per* induction *in vivo* appeared to be slightly faster than in slices (Figs. 3, 4). Importantly, peripheral treatment with OXM also altered the diurnal expression rhythms of genes involved in regulating liver carbohydrate metabolism which may underline the metabolic effects of daytime feeding in rodents (Fig. 5). Similar to the OXM effects on clock gene expression (Figs. 3, 4), refeeding acutely induces hepatic *Per1/2* expression, which has been proposed as an integral part of the food-driven clock-resetting mechanism (15, 47). In our study, we demonstrated that food intake after overnight fasting stimulated OXM secretion and led to hepatic up-regulation of *Per* expression, which was blocked by OXM neutralization in the circulation. Accordingly, liver slice cultures from re-fed *Per2::LUC* reporter mice showed food-dependent phase delays and these effects were attenuated by OXM neutralization (Fig. 6). OXM neutralization does not completely inhibit the effects of refeeding on *Per* induction and liver clock resetting. This might be due to incomplete neutralization of OXM, or the contribution of other food-induced factors as discussed above. Of note, while our data do not provide evidence for a direct involvement of GLP-1(R), it has been suggested that postprandial GLP-1 signaling may indirectly affect liver clock phase (31).

Our data indicate an involvement of OXM signaling in food-driven resetting of the liver circadian clock. Similar to what was previously reported in humans (48), we detected elevated OLI levels in fed as compared to starved mice and in response to acute food intake (Fig. 6). The diurnal variability of OLI under *ad libitum* feeding conditions was moderate, but fasting resulted in an approximate 20% reduction of diurnal OLI secretion. Together this indicates that small meals as consumed during the inactive phase affect OXM secretion, but that substantial food intake is necessary to acutely increase OXM secretion to an extent sufficient to affect the liver clock. Of note, interpretation of plasma OXM blood levels is difficult as many OXM assays exhibit some degree of cross-reactivity with glucagon and the closely related glicentin. Glicentin differs from OXM only by a 32-amino acid N-terminal extension (IP-1; Fig. 1) and is released from the gut

after food intake at approximately similar levels (49, 50), thus we cannot exclude the possibility that glicentin may exhibit actions that overlap with those described for OXM.

In summary, we show that food intake induces OLI blood levels and hepatic clock resetting in mice. OXM treatment mimics food-mediated clock resetting in slices and *in vivo* in a time of day-dependent manner. Food is a major regulator of hepatic transcriptome rhythms (37). A role for metabolic hormones, e.g. insulin, glucagon, or glucocorticoids, in the regulation of peripheral clocks has been suggested (15, 18, 25). However, the mechanisms of food-related synchronization of peripheral clocks and their uncoupling from the SCN under time-restricted food intake rhythms are still poorly understood. Our data suggest that OXM – most likely in concert with other gut- and pancreas-derived hunger- or satiety-signaling peptides – is involved in the detrimental effects of mistimed food intake on metabolic homeostasis (3, 11, 12). While interfering with insulin signaling may be clinically problematic because of its potential deleterious effects on glycemia, chronotherapeutic targeting of peripheral incretin signaling may provide an alternative therapeutic strategy against metabolic disorders arising from circadian strain as observed in shift workers or during jetlag.

Materials and Methods:

Animal strains

All animal experiments were ethically assessed and licensed by the Office of Consumer Protection and Food Safety of the State of Lower Saxony and in accordance with the German Law of Animal Welfare (license nos. V312-7224.122-4 and 33.12-42502-04-12/0893). For all experiments adult wild-type mice male C57BL/6J (8-24 weeks old) were used. If not stated otherwise, mice were provided with food and water *ad libitum*. To investigate the effect of OXM on gene expression by qPCR or *in situ* hybridization, mice were peripherally treated with OXM (*i.v.* 4 µg/mouse; *i.p.* 25 µg/mouse) or vehicle (PBS) at ZT3, ZT15, or 12 hours after light-off. For luminescence measurements adult heterozygous males *Per2::LUC* (24) and *Per2::LUC* x *Glp1r*$^{-/-}$ were used. *Glp1r*$^{-/-}$ mice were maintained on a C57B/6J background (51). All mice were exposed to a 12-hr: 12-hr light-dark cycle with 100 lux in the light phase (LD12:12). Animals were sacrificed at indicated time points by cervical dislocation. Animals euthanized during the dark phase were handled under red light and eyes were removed before dissection. All tissue samples were collected and immediately snap-frozen on dry ice or liquid nitrogen. For long-term storage tissues were kept at -80°C.

Refeeding experiments

In order to test *Per* induction and phase shifts after refeeding, mice were fasted for one night (13 hours, or from ZT12 – ZT1) and either food deprived until decapitation or refed at ZT1. The refed mice received either *anti*-OXM rabbit IgG (*i.p.* 50 µg/mouse; Bachem T-4800) or control IgG from unimmunized rabbit serum (Sigma I5006) at ZT1 when food was returned.

Liver slice cultures and peptide treatments

Luminescence was measured from cultured liver slices of heterozygous *Per2::LUC* mice as described previously (24) modified to include the use of culture plate inserts (Millipore, Billerica, MA). Briefly, the median lobe of the liver was isolated and 300 µm slices were prepared using a vibratome (Campden Instruments, Loughborough, UK). The slices were immediately placed onto a culture plate insert in 35 mm petri dishes filled with 1 ml culture medium (D-MEM with high glucose, w/o L-glutamine & phenol red; Invitrogen) supplemented with 3 mM sodium carbonate (Sigma-Aldrich), 10 mM HEPES buffer, 2 mM L-glutamine, 2 % B-27 supplement, 25 U/ml penicillin/streptomycin and 0.1 mM D-luciferin (all Life Technologies). Luminescence was measured in a luminometer (Actimetrics) at 32.5 °C with 5% CO_2. Analyses were performed using the LumiCycle analysis (Actimetrics) and Prism software packages (GraphPad, La Jolla, CA). PER2::LUC activity in slices closely follows a sine wave shape. The intersection of the ascending cross-section of the sine wave with the x-axis was defined as 0°/360°, the peak as 90°. Degrees at the time point of treatment were calculated as follows: $T_p\ [°] = ((T_p\ [hsm] - P_{bt}\ [hsm])\ :\ P_{bt})\ \text{x}\ 360 + 90$ with T_p = treatment phase; ° = degree; hsm = hours after start of measurement; P_{bt} = peak before treatment. If the result was > 360° the value was subtracted by 360. Raw data were baseline subtracted with running averages of 24 h. Peaks were defined as middle time point between two troughs of the sine wave. Period was determined as the time between peaks averaged over 2-3 consecutive cycles. For the duration of treatment samples were maintained at 32.5°C to avoid resetting of clock gene expression rhythms due to temperature changes. Phase shifts were determined by comparing extrapolated peak times from sine wave fits before and after treatment. Unless otherwise stated, peptides used for experiments were dissolved in culture medium and administered at a final concentration of 450 pM.

Quantitative real-time (qPCR)

Quantitative real-time PCR (qPCR) was performed with a CFX96 thermocycler system (Bio-Rad, Munich, DE) with iQ-SYBR Green SuperMix (Bio-Rad). Relative quantification of expression

levels by a modified ΔΔCT calculation was performed as described (52). *ß-Actin* was used as a reference gene. Statistical analyses were performed using GraphPad Prism software. Circadian profiles of clock gene expression were normalized against the average values over all time points. Induction analyses were normalized against untreated conditions (0 min). PCR primer sequences are listed in Fig. 6 – source data 1.

In situ hybridization (ISH)

The *Per1* probe corresponds to nucleotides 1 to 619 (GenBank accession number AF022992) and *Per2* corresponds to nucleotides 229 to 768 of GenBank AF036893. PCR products had been cloned into *pCR II TOPO* vector using TOPO TA Cloning Kit (Life Technologies) (53). Linearization of vectors for *in vitro* transcription was done with EcoRI. ^{35}S-UTP (PerkinElmer) labeled RNA probes were prepared using RNA Transcription Kit (Maxi Script Labeling Kit, Life Technologies) with T7 or T3 RNA polymerases according to the manufacturer's protocol. 10 µm cryosections were cut using a Leica CM3050 cryostat. Cryosections were fixed in 4 % paraformaldehyde, acetylated in acetic anhydride and dehydrated with ethanol. Hybridization was performed over night at 55-58°C. Autoradiographs were analyzed by densitometry (Bio-Rad GS-800) using QuantityOne software (Bio-Rad). Three sections per brain were used and background values were calculated from adjacent tissue areas on the same slide for each section. Measurements from different animals/experiments were compared for statistical analysis using GraphPad Prism (GraphPad).

Chromatin immunoprecipiation (ChIP)

Liver slices were homogenized and immediately cross linked with 1% formaldehyde. Chromatin was sonicated for 15-s on/20-s off cycles for 22 min using a Bioruptor sonicator (Diagenode). Samples were incubated overnight at 4 °C with CREB antibody (ab31387, Abcam). After clearing, samples were incubated with A/G agarose beads (Thermo Scientific) for 1 h at 4 °C

followed by repetitive washings. After boiling for 10 min in 10 % Chelex (Bio-Rad) with Proteinase K (150 mg/mL) samples were spun down and DNA-containing supernatant was collected for PCR. qPCR was performed as described above, and values were normalized to percentage of input. Primer sequences were: 5′-CAGCTGCCTCGCCCCGCCTC-3′ / 5′-CCCAAGCAGCCATTGCTCGC-3′ (Per1 CRE) and 5’-CCCCGCAGTCCTACGGTGCTG-3’ / 5’-AAGCCCCCAAACAACTGAAGGT-3’ (500 bp downstream sequence).

Hormone measurements

Blood collection for radioimmunoassay (RIA) was performed at ZT1 after 12 h fast. Mice were allowed to recover for 3 days, then fasted again followed by treatments (with or without refeeding). Blood was collected from the tail vein at 0 min, 20 min, 60 min and 120 min after treatment. Plasma concentrations of OLI were determined by RIA (Phoenix Pharmaceutics, Karlsruhe, DE) according to manufacturer’s protocol modified to use a 50% reaction volume. GLP-1 (EZGLP-1T-36K, Millipore), insulin (Catalog# 90080, CrystalChem, Downers Grove, IL), and GCG plasma levels (EZGLU-30K, Millipore) were determined by ELISA according to the manufacturers’ protocols.

Statistics

Data were analyzed with GraphPad Prism (GraphPad, LaJolla, CA). Mann-Whitney tests were used for simple comparisons. For dose responses one-way ANOVAs and for two-factor comparisons two-way ANOVAs with Bonferroni post-tests were used. A p-value of less than 0.05 was considered significant.

Acknowledgments:

Author contributions: DL, AHT, AL, JLB, CK, and HO performed experiments and revised the manuscript. DJD contributed reagents, discussions, and revised the manuscript. DL, AHT, CK & HO analyzed data and wrote the paper.

Thanks: The authors thank Bernard Thorens, University of Lausanne for indirectly providing *Glp1r-/-* mice, Nadine Naujokat and Christin Helbig for technical assistance, and David K. Welsh, UC San Diego, and Gregor Eichele, Max Planck Institute for Biophysical Chemistry Göttingen, for critical comments on the manuscript.

Funding: HO is a Lichtenberg Fellow of the Volkswagen Foundation. This work was supported by a DFG research grant (TR-SFB134). DJD is supported by the Canada Research Chairs Program, a Banting and Best Diabetes Centre Novo Nordisk Chair in Incretin Biology, and CIHR grant 93749.

Competing interests:

The authors declare that they have no competing interests.

References:

1. Herichova I. Changes of physiological functions induced by shift work. Endocr Regul. 2013 Jul;47(3):159-70. PubMed PMID: 23889486. Epub 2013/07/31. eng.
2. Rosenberg R, Doghramji PP. Is shift work making your patient sick? Emerging theories and therapies for treating shift work disorder. Postgrad Med. 2011 Sep;123(5):106-15. PubMed PMID: 21904092.
3. Albrecht U. Timing to perfection: the biology of central and peripheral circadian clocks. Neuron. 2012 Apr 26;74(2):246-60. PubMed PMID: 22542179.
4. Takahashi JS, Hong HK, Ko CH, McDearmon EL. The genetics of mammalian circadian order and disorder: implications for physiology and disease. Nat Rev Genet. 2008 Oct;9(10):764-75. PubMed PMID: 18802415. Epub 2008/09/20. eng.
5. Yan J, Wang H, Liu Y, Shao C. Analysis of gene regulatory networks in the mammalian circadian rhythm. PLoS computational biology. 2008 Oct;4(10):e1000193. PubMed PMID: 18846204. Pubmed Central PMCID: 2543109.
6. Golombek DA, Rosenstein RE. Physiology of circadian entrainment. Physiol Rev. 2010 Jul;90(3):1063-102. PubMed PMID: 20664079.
7. Dibner C, Schibler U, Albrecht U. The mammalian circadian timing system: organization and coordination of central and peripheral clocks. Annual review of physiology. 2010 Mar 17;72:517-49. PubMed PMID: 20148687. Epub 2010/02/13. eng.
8. Stokkan KA, Yamazaki S, Tei H, Sakaki Y, Menaker M. Entrainment of the circadian clock in the liver by feeding. Science. 2001 Jan 19;291(5503):490-3. PubMed PMID: 11161204.
9. Damiola F, Le Minh N, Preitner N, Kornmann B, Fleury-Olela F, Schibler U. Restricted feeding uncouples circadian oscillators in peripheral tissues from the central pacemaker in the suprachiasmatic nucleus. Genes Dev. 2000 Dec 1;14(23):2950-61. PubMed PMID: 11114885.

10. Lowden A, Moreno C, Holmback U, Lennernas M, Tucker P. Eating and shift work - effects on habits, metabolism and performance. Scandinavian journal of work, environment & health. 2010 Mar;36(2):150-62. PubMed PMID: 20143038.

11. Arble DM, Bass J, Laposky AD, Vitaterna MH, Turek FW. Circadian timing of food intake contributes to weight gain. Obesity (Silver Spring). 2009 Nov;17(11):2100-2. PubMed PMID: 19730426. Pubmed Central PMCID: 3499064.

12. Hatori M, Vollmers C, Zarrinpar A, DiTacchio L, Bushong EA, Gill S, et al. Time-restricted feeding without reducing caloric intake prevents metabolic diseases in mice fed a high-fat diet. Cell metabolism. 2012 Jun 6;15(6):848-60. PubMed PMID: 22608008. Epub 2012/05/23. eng.

13. Barclay JL, Husse J, Bode B, Naujokat N, Meyer-Kovac J, Schmid SM, et al. Circadian desynchrony promotes metabolic disruption in a mouse model of shiftwork. PLoS One. 2012;7(5):e37150. PubMed PMID: 22629359. Pubmed Central PMCID: 3357388.

14. Antunes LC, Levandovski R, Dantas G, Caumo W, Hidalgo MP. Obesity and shift work: chronobiological aspects. Nutrition research reviews. 2010 Jun;23(1):155-68. PubMed PMID: 20122305.

15. Tahara Y, Otsuka M, Fuse Y, Hirao A, Shibata S. Refeeding after fasting elicits insulin-dependent regulation of Per2 and Rev-erbalpha with shifts in the liver clock. Journal of biological rhythms. 2011 Jun;26(3):230-40. PubMed PMID: 21628550. Epub 2011/06/02. eng.

16. Chaves I, van der Horst GT, Schellevis R, Nijman RM, Koerkamp MG, Holstege FC, et al. Insulin-FOXO3 signaling modulates circadian rhythms via regulation of clock transcription. Curr Biol. 2014 Jun 2;24(11):1248-55. PubMed PMID: 24856209.

17. LeSauter J, Hoque N, Weintraub M, Pfaff DW, Silver R. Stomach ghrelin-secreting cells as food-entrainable circadian clocks. Proc Natl Acad Sci U S A. 2009 Aug 11;106(32):13582-7. PubMed PMID: 19633195. Pubmed Central PMCID: 2726387.

18. Sun X, Dang F, Zhang D, Yuan Y, Zhang C, Wu Y, et al. Glucagon-CREB/CRTC2 Signaling Cascade Regulates Hepatic BMAL1. J Biol Chem. 2014 Dec 5. PubMed PMID: 25480789.

19. Hirao A, Tahara Y, Kimura I, Shibata S. A balanced diet is necessary for proper entrainment signals of the mouse liver clock. PLoS One. 2009;4(9):e6909. PubMed PMID: 19738906. Pubmed Central PMCID: 2734168.

20. Stanley S, Wynne K, McGowan B, Bloom S. Hormonal regulation of food intake. Physiol Rev. 2005 Oct;85(4):1131-58. PubMed PMID: 16183909.

21. Drucker DJ. Biologic actions and therapeutic potential of the proglucagon-derived peptides. Nature clinical practice Endocrinology & metabolism. 2005 Nov;1(1):22-31. PubMed PMID: 16929363.

22. Baldissera FG, Holst JJ, Knuhtsen S, Hilsted L, Nielsen OV. Oxyntomodulin (glicentin-(33-69)): pharmacokinetics, binding to liver cell membranes, effects on isolated perfused pig pancreas, and secretion from isolated perfused lower small intestine of pigs. Regulatory peptides. 1988 May;21(1-2):151-66. PubMed PMID: 2839871.

23. Gros L, Thorens B, Bataille D, Kervran A. Glucagon-like peptide-1-(7-36) amide, oxyntomodulin, and glucagon interact with a common receptor in a somatostatin-secreting cell line. Endocrinology. 1993 Aug;133(2):631-8. PubMed PMID: 8102095.

24. Yoo SH, Yamazaki S, Lowrey PL, Shimomura K, Ko CH, Buhr ED, et al. PERIOD2::LUCIFERASE real-time reporting of circadian dynamics reveals persistent circadian oscillations in mouse peripheral tissues. Proc Natl Acad Sci U S A. 2004 Apr 13;101(15):5339-46. PubMed PMID: 14963227.

25. Balsalobre A, Brown SA, Marcacci L, Tronche F, Kellendonk C, Reichardt HM, et al. Resetting of circadian time in peripheral tissues by glucocorticoid signaling. Science. 2000 Sep 29;289(5488):2344-7. PubMed PMID: 11009419. Epub 2000/09/29. eng.

26. Le Quellec A, Kervran A, Blache P, Ciurana AJ, Bataille D. Oxyntomodulin-like immunoreactivity: diurnal profile of a new potential enterogastrone. J Clin Endocrinol Metab. 1992 Jun;74(6):1405-9. PubMed PMID: 1592887.

27. Jorgensen R, Kubale V, Vrecl M, Schwartz TW, Elling CE. Oxyntomodulin differentially affects glucagon-like peptide-1 receptor beta-arrestin recruitment and signaling through Galpha(s). J Pharmacol Exp Ther. 2007 Jul;322(1):148-54. PubMed PMID: 17395766.

28. Sinclair EM, Yusta B, Streutker C, Baggio LL, Koehler J, Charron MJ, et al. Glucagon receptor signaling is essential for control of murine hepatocyte survival. Gastroenterology. 2008 Dec;135(6):2096-106. PubMed PMID: 18809404.

29. Campos RV, Lee YC, Drucker DJ. Divergent tissue-specific and developmental expression of receptors for glucagon and glucagon-like peptide-1 in the mouse. Endocrinology. 1994 May;134(5):2156-64. PubMed PMID: 8156917.

30. Dunphy JL, Taylor RG, Fuller PJ. Tissue distribution of rat glucagon receptor and GLP-1 receptor gene expression. Mol Cell Endocrinol. 1998 Jun 25;141(1-2):179-86. PubMed PMID: 9723898.

31. Panjwani N, Mulvihill EE, Longuet C, Yusta B, Campbell JE, Brown TJ, et al. GLP-1 receptor activation indirectly reduces hepatic lipid accumulation but does not attenuate development of atherosclerosis in diabetic male ApoE(-/-) mice. Endocrinology. 2013 Jan;154(1):127-39. PubMed PMID: 23183176.

32. Gonzalez GA, Montminy MR. Cyclic AMP stimulates somatostatin gene transcription by phosphorylation of CREB at serine 133. Cell. 1989 Nov 17;59(4):675-80. PubMed PMID: 2573431.

33. Dalle S, Longuet C, Costes S, Broca C, Faruque O, Fontes G, et al. Glucagon promotes cAMP-response element-binding protein phosphorylation via activation of ERK1/2 in MIN6 cell line and isolated islets of Langerhans. J Biol Chem. 2004 May 7;279(19):20345-55. PubMed PMID: 14988413.

34. Welsh DK, Takahashi JS, Kay SA. Suprachiasmatic nucleus: cell autonomy and network properties. Annu Rev Physiol. 2010;72:551-77. PubMed PMID: 20148688. Pubmed Central PMCID: 3758475.

35. Lamia KA, Storch KF, Weitz CJ. Physiological significance of a peripheral tissue circadian clock. Proc Natl Acad Sci U S A. 2008 Sep 30;105(39):15172-7. PubMed PMID: 18779586. Epub 2008/09/10. eng.

36. Salgado-Delgado R, Angeles-Castellanos M, Saderi N, Buijs RM, Escobar C. Food intake during the normal activity phase prevents obesity and circadian desynchrony in a rat model of night work. Endocrinology. 2010 Mar;151(3):1019-29. PubMed PMID: 20080873. Epub 2010/01/19. eng.

37. Vollmers C, Gill S, DiTacchio L, Pulivarthy SR, Le HD, Panda S. Time of feeding and the intrinsic circadian clock drive rhythms in hepatic gene expression. Proceedings of the National Academy of Sciences of the United States of America. 2009 Dec 15;106(50):21453-8. PubMed PMID: 19940241. Pubmed Central PMCID: 2795502. Epub 2009/11/27. eng.

38. Akhtar RA, Reddy AB, Maywood ES, Clayton JD, King VM, Smith AG, et al. Circadian cycling of the mouse liver transcriptome, as revealed by cDNA microarray, is driven by the suprachiasmatic nucleus. Curr Biol. 2002 Apr 2;12(7):540-50. PubMed PMID: 11937022.

39. Miller BH, McDearmon EL, Panda S, Hayes KR, Zhang J, Andrews JL, et al. Circadian and CLOCK-controlled regulation of the mouse transcriptome and cell proliferation. Proc Natl Acad Sci U S A. 2007 Feb 27;104(9):3342-7. PubMed PMID: 17360649. Pubmed Central PMCID: 1802006.

40. Kornmann B, Preitner N, Rifat D, Fleury-Olela F, Schibler U. Analysis of circadian liver gene expression by ADDER, a highly sensitive method for the display of differentially expressed mRNAs. Nucleic Acids Res. 2001 Jun 1;29(11):E51-1. PubMed PMID: 11376163.

553 41. Yamajuku D, Inagaki T, Haruma T, Okubo S, Kataoka Y, Kobayashi S, et al. Real-time
554 monitoring in three-dimensional hepatocytes reveals that insulin acts as a synchronizer for
555 liver clock. Sci Rep. 2012;2:439. PubMed PMID: 22666542. Pubmed Central PMCID:
556 3365280. Epub 2012/06/06. eng.
557 42. Dunlap JC. Molecular bases for circadian clocks. Cell. 1999 Jan 22;96(2):271-90. PubMed
558 PMID: 9988221. Epub 1999/02/13. eng.
559 43. Lowrey PL, Takahashi JS. Mammalian circadian biology: elucidating genome-wide levels
560 of temporal organization. Annu Rev Genomics Hum Genet. 2004;5:407-41. PubMed
561 PMID: 15485355. Epub 2004/10/16. eng.
562 44. Balsalobre A, Damiola F, Schibler U. A serum shock induces circadian gene expression in
563 mammalian tissue culture cells. Cell. 1998 Jun 12;93(6):929-37. PubMed PMID: 9635423.
564 45. Albrecht U, Sun ZS, Eichele G, Lee CC. A differential response of two putative mammalian
565 circadian regulators, mper1 and mper2, to light. Cell. 1997 Dec 26;91(7):1055-64. PubMed
566 PMID: ISI:000071281400021. English.
567 46. Yan L, Silver R. Differential induction and localization of mPer1 and mPer2 during
568 advancing and delaying phase shifts. Eur J Neurosci. 2002 Oct;16(8):1531-40. PubMed
569 PMID: 12405967. Pubmed Central PMCID: 3281755.
570 47. Oike H, Nagai K, Fukushima T, Ishida N, Kobori M. Feeding cues and injected nutrients
571 induce acute expression of multiple clock genes in the mouse liver. PLoS One.
572 2011;6(8):e23709. PubMed PMID: 21901130. Pubmed Central PMCID: 3162004.
573 48. Mayo KE, Miller LJ, Bataille D, Dalle S, Goke B, Thorens B, et al. International Union of
574 Pharmacology. XXXV. The glucagon receptor family. Pharmacol Rev. 2003 Mar;55(1):167-
575 94. PubMed PMID: 12615957.
576 49. Tang-Christensen M, Vrang N, Larsen PJ. Glucagon-like peptide containing pathways in
577 the regulation of feeding behaviour. Int J Obes Relat Metab Disord. 2001 Dec;25 Suppl
578 5:S42-7. PubMed PMID: 11840214.

50. Blache P, Kervran A, Bataille D. Oxyntomodulin and glicentin: brain-gut peptides in the rat. Endocrinology. 1988 Dec;123(6):2782-7. PubMed PMID: 3197645.

51. Scrocchi LA, Brown TJ, MaClusky N, Brubaker PL, Auerbach AB, Joyner AL, et al. Glucose intolerance but normal satiety in mice with a null mutation in the glucagon-like peptide 1 receptor gene. Nat Med. 1996 Nov;2(11):1254-8. PubMed PMID: 8898756.

52. Pfaffl MW. A new mathematical model for relative quantification in real-time RT-PCR. Nucleic Acids Res. 2001 May 1;29(9):e45. PubMed PMID: 11328886. Epub 2001/05/09. eng.

53. Oster H, Yasui A, van der Horst GT, Albrecht U. Disruption of mCry2 restores circadian rhythmicity in mPer2 mutant mice. Genes Dev. 2002 Oct 15;16(20):2633-8. PubMed PMID: 12381662.

Figure legends:

Fig. 1. OXM phase- and dose-dependently resets circadian clocks in liver slices. (**A**) Schematic sequence of the proglucagon-derived peptides (GRPP – glicentin-related pancreatic peptide; GLIC – glicentin; OXM – oxyntomodulin; GCG – glucagon; IP-1 – intervening peptide-1; GLP-1 – glucagon-like peptide-1; IP-2 – intervening peptide-2; GLP-2 – glucagon-like peptide -2). (**B-F**) Example luminescence traces and dose-dependent responses for GLP-1 (**B**; $F(6,28)=1.509$), GLP-2 (**C**; $F(6,28)=1.530$), GRPP (**D**; $F(6,28)=1.151$), GCG (**E**; $F(6,28)=3.569$), and OXM (**F**; $F(6,28)=8.790$) induced phase resetting of PER2::LUC rhythms in liver slices treated at 180-200°. Data are presented as mean ± S.E.M. (n=5). One-way ANOVA (F-values with degrees of freedom provided in brackets): *, $P < 0.05$; **, $P < 0.01$; ***, $P < 0.001$. Asterisks indicate significant differences relative to PBS treatment (white bars). (**G**) Phase response curve for OXM-induced phase resetting of PER2::LUC rhythms in liver slices. Circles: raw data of individual slices; dashed line: sine wave regression with harmonics.

Fig. 1 – fig. suppl. 1. Phase response curve for dexamethasone (DEX) treatment in *Per2::LUC* liver slice cultures. Black dots: phase shifts of individual DEX treatments (100 µM); dashed line: sine wave regression with first and second order harmonics (CircWave).

Fig. 1 – source data 1. Table of effects of metabolic peptide treatment on PER2::LUC liver slice rhythms.

Fig. 2. Glucagon receptor regulates phase resetting effects of OXM and GCG in *Per2::LUC* liver slices. (**A**) OXM induced phase shifts in *Per2::LUC* and *Per2::LUC* x *Glp1r*$^{-/-}$ liver slices. Mann-Whitney test: ## $P < 0.01$ against solvent. (**B**) GCG and OXM-induced phase shifts in *Per2::LUC* slices are abolished by co-treatment with GRI-2. One-way ANOVA with Bonferroni

post-test: P <0.05; ### P < 0.001 against solvent; * P < 0.05; *** P < 0.001. Data are presented as mean ± S.E.M. (n=8); F(7, 56)=7.314. (**C**) OXM treatment promotes binding of CREB to CRE elements at the *Per1* gene promoter. One-way ANOVA with Bonferroni post-test: *** P < 0.001 against 0'. Data are presented as mean ± S.E.M. (n=5; F(5, 24)=22.2).

Fig. 2 – fig. suppl. 1. Absence of *Glp1r* transcripts in mouse liver. RT-PCR with different primer sets targeting all annotated coding exons of the murine *Glp1r* gene. Exon 1 was not tested, as it mainly contains non-coding poly-C- and poly-G-rich sequences, which precludes specific primer design. cDNA preparations from wild type livers were tested (lane 2). Wild-type pancreas cDNA was chosen as positive (lane 4) and liver cDNA from *Glp1r*-deficient mice and water as negative controls (lanes 3 and 5). Lane 1: 100-bp DNA ladder.

Fig. 3. OXM treatment induces *Per1/2* expression in organotypic liver slices. (**A-C**) WT liver slices were treated with OXM (grey) or vehicle (PBS; black) at 180° and analyzed for clock gene expression of *Per1* (**A**; factor treatment F(1, 40)=0.785; time F(3,40)=34.95; interaction F(3,40)=16.33), *Per2* (**B**; factor treatment F(1, 40)=24.02; time F(3,40)=29.4; interaction F(3,40)=38.38) and *Bmal1* (**C**; factor treatment F(1, 40)=0.108; time F(3,40)=17.39; interaction F(3,40)=3.607) by qPCR. (**D-F**) WT liver slices were treated with OXM (grey) or PBS (black) at 360° and analyzed for expression of *Per1* (**D**; factor treatment F(1, 40)=1.179; time F(3,40)=36.33; interaction F(3,40)=1.349), *Per2* (**E**; factor treatment F(1, 40)=5.757; time F(3,40)=13.57; interaction F(3,40)=1.135) and *Bmal1* (**F**; factor treatment F(1, 40)=4.112; time F(3,40)=8.788; interaction F(3,40)=0.491) by qPCR. (**G, H**) OXM-induced *Per1/2* expression is retained in *Glp1r*$^{-/-}$ liver slices. *Per1*: factor treatment F(1, 42)=8.48; time F(2, 42)=10.95; interaction F(2,42)=0.525. *Per2*: factor treatment F(1 ,42)=10.5; time F(2, 42)=3.662; interaction F(2, 42)=5.845. *Glp1r*$^{-/-}$ liver slices were treated as described for WT above. Data are presented

as mean ± S.E.M. (n=6 for WT and 8 for *Glp1r*$^{-/-}$). Two-way ANOVA with Bonferroni post-test: **, P < 0.01; ***, P < 0.001.

Fig. 4. OXM treatment induces *Per1/2* expression and resets the liver circadian clock *in vivo*. (**A, B**) Hepatic *Per* gene expression after OXM (grey) or vehicle (PBS; black) *i.v.* injection at ZT3 (**A**) and ZT15 (**B**). ZT3: *Per1*: factor treatment F(1, 24)=5.695; time F(2, 24)=34.74; interaction F(2, 24)=4.965; *Per2*: factor treatment F(1, 24)=64.84; time F(2, 24)=9.381; interaction F(2, 24)=6.915. ZT15: *Per1*: factor treatment F(1, 12)=1.096; time F(2, 12)=0.005; interaction F(2, 12)=1.367; *Per2*: factor treatment F(1, 24)=0.255; time F(2, 24)=0.001; interaction F(2, 24)=1.172. (**C**) SCN signal after *in situ* hybridization (ISH) of brain sections with ^{35}S-labelled antisense probes for *Per1/2* 30 min after OXM/PBS treatment at ZT3 in the same animals used in (**A**). Left panel: representative autoradiograph scans containing the SCN; right panel: quantification of the ISH. (**D**) Resetting of *Per2* and *Dbp* rhythms in livers of wild-type mice after an *i.p.* injection of either OXM (grey) or vehicle (PBS; black) after 12 h darkness; *Per2*: factor treatment F(1, 24)=5.531; time F(5, 24)=46.37; interaction F(5, 24)=18.71. *Dbp*: factor treatment F(1, 24)=0.094; time F(5, 24)=119.2; interaction F(5, 24)=38.58. All data are presented as mean ± S.E.M. (n=3-5). A, B and D: two-way ANOVA with Bonferroni post-test: *, P < 0.05, **, P < 0.01; ***, P < 0.001; C: Mann-Whitney test.

Fig. 5. OXM treatment modulates diurnal expression profile of hepatic genes involved in liver carbohydrate metabolism. (**A-F**) Relative gene expression of *Foxo1* (**A**; factor treatment F(1, 24)=0.001, time F(5, 24)=5.547, interaction F(5, 24)=11.13), *Pdk4* (**B**; factor treatment F(1, 24)=0.197, time F(5, 24)=3.35, interaction F(5, 24)=3.247), *Pklr* (**C**; factor treatment F(1, 24)=11.63, time F(5, 24)=5.61, interaction F(5, 24)=3.61), *Pepck* (**D**; factor treatment F(1, 24)=0.574, time F(5, 24)=2.043, interaction F(5, 24)=0.299), the glucose transporter *Slc2a2* (**E**; factor treatment F(1, 24)=2.582, time F(5, 24)=15.98, interaction F(5, 24)=2.642) and the

669 pyruvate transporter *Slc16a7* (**F**; factor treatment F(1, 24)=1.539, time F(5, 24)=7.472,
670 interaction F(5, 24)=6.586) after ***i.p.*** administration of either OXM (grey) or vehicle (PBS; black)
671 after 12 h in darkness. Data are presented as mean ± S.E.M. (n=4). Two-way ANOVA with
672 Bonferroni post-test: *, $P < 0.05$, **, $P < 0.01$; ***, $P < 0.001$.
673
674 **Fig. 6.** Endogenous OXM signaling regulates food intake-mediated resetting of the liver
675 circadian clock. (**A**) Plasma OLI diurnal profiles under *ad libitum* food and fasting conditions.
676 Data are presented as mean ± S.E.M (n=6); factor time F(5,60)=0.628, feeding condition
677 F(1,60)=15.37, interaction F(5,60)=0.638. Grey shading indicates the dark phase. (**B**) OLI levels
678 show high individual variations in mice after 12 h of food deprivation (ZT13-1). (**C**) Plasma OLI
679 (normalized to individual fasting levels) after refeeding (grey line) or under continuous starving
680 (black line); factor time F(3,21)=3.544, feeding condition F(1,21)=15.82, interaction
681 F(3,21)=4.717. (**D**) Liver *Per1/2* induction following fasting-refeeding determined by qPCR;
682 *Per1*: factor time F(3,25)=0.454, feeding condition F(1,25)=1.376, interaction F(3,25)=4.453;
683 *Per2*: factor time F(3,25)=6.938, feeding condition F(1,25)=38.48, interaction F(3,25)=3.767. (**E**)
684 WT and (**F**) *Glp1r*$^{-/-}$ liver *Per1/2* expression after fasting-refeeding with control IgG injection
685 (grey) or OXM immuno-neutralization by *anti*-OXM IgG (aOXM) injection at ZT0; WT: *Per1*:
686 F(2,12)=71.76, *Per2*: F(2,12)=47.41; *Glp1r*$^{-/-}$: *Per1* F(2,12)=11.51, *Per2*: F(2,12)=5.585. (**G-I**)
687 Treatment with *anti*-OXM IgG does not affect postprandial regulation of insulin, GLP-1, and
688 GCG. Plasma levels of insulin (**G**; F(2, 12)=17.44), GLP-1 (**H**; F(2, 12)=5.563), and GCG (**I**;
689 F(2, 12)=7.128) after fasting-refeeding with control IgG injection (grey) or OXM immuno-
690 neutralization by *anti*-OXM IgG (aOXM) treatment at ZT0. One- (**E-I**) or two-way ANOVA (**A,**
691 **C, D**) with Bonferroni post-test: *, $P < 0.05$; **, $P < 0.01$; ***, $P < 0.001$ against fasted; ##, $p <$
692 0.01; ### $p < 0.001$ against IgG. Data are presented as mean ± S.E.M (n=5). (**J, K**) Liver
693 PER2::LUC rhythms after fasting-refeeding with control IgG or αOXM administration. (**J**)
694 Representative luminescence traces. (**K**) Comparison of phases (2nd peak in culture) after

refeeding and/or *anti*-OXM treatment (Data are presented as mean ± S.E.M (n = 4 mice per condition, an average of 3 slice preparations of each mouse were used); two-way ANOVA with Bonferroni post-test: *, $P < 0.05$ against fasted; factor treatment $F(1, 12)=5.127$, feeding condition $F(1, 12)=13.02$, interaction $F(1, 12)=5.044$).

Fig. 6 – fig. suppl. 1. Time course of OLI plasma levels after OXM injection. Time course of OLI appearance in plasma following *i.v.* (4 µg) or *i.p.* (25 µg) injections of OXM. OLI plasma level changes are expressed relative to starving levels (0 min) for each individual. Data are presented as mean ± SEM (n=5). 2-way ANOVA with Bonferroni post-test: ***, $P < 0.001$; factor treatment $F(2, 48)=9.014$, feeding condition $F(3, 48)=4.95$, interaction $F(6, 48)=5.698$.

Fig. 6 – source data 1. Primer sequences for PCR reactions.

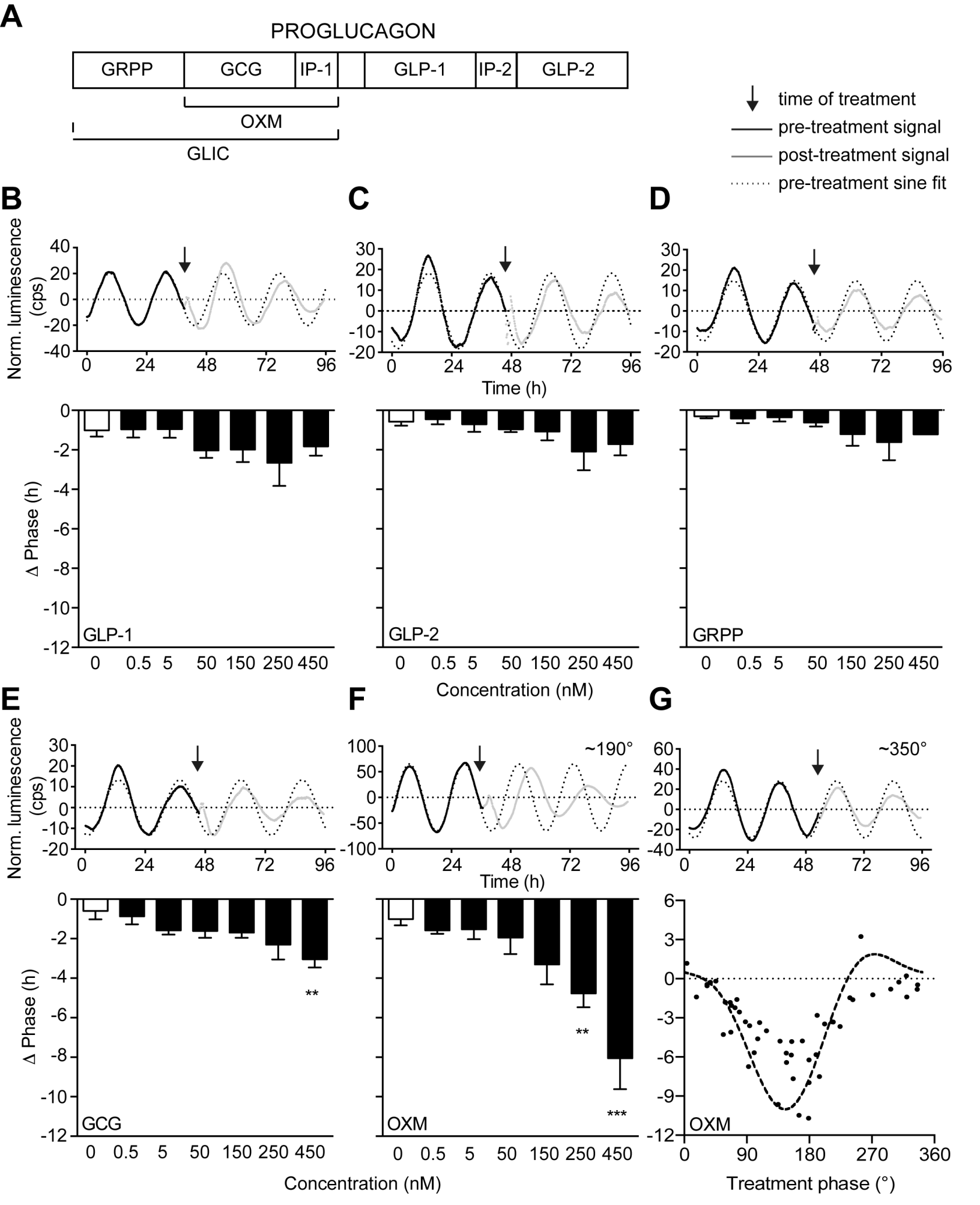
A
PROGLUCAGON
GRPP
GCG
IP-1
GLP-1
IP-2
GLP-2
OXM
GLIC
time of treatment
pre-treatment signal
post-treatment signal
pre-treatment sine fit
B
C
D
Norm. luminescence (cps)
Time (h)
Δ Phase (h)
GLP-1
GLP-2
GRPP
Concentration (nM)
E
F
G
~190°
~350°
GCG
OXM
**
***
Treatment phase (°)

OXM Figure 1

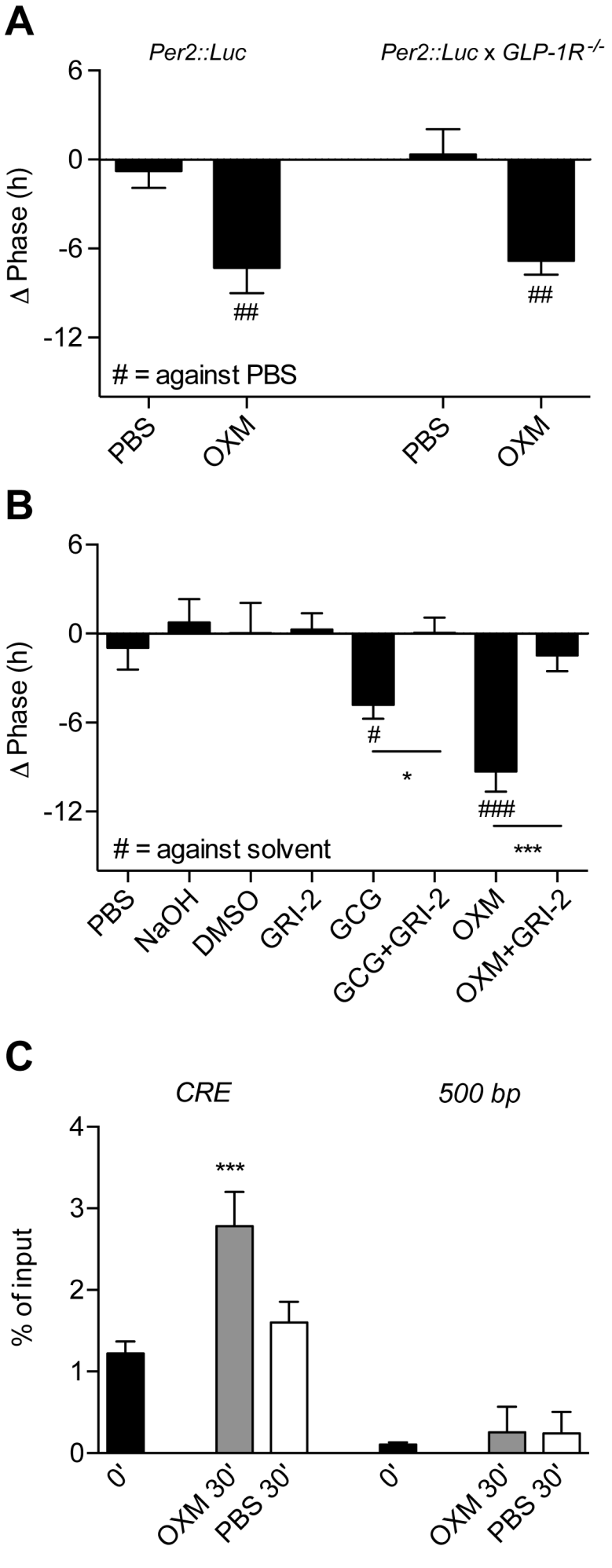
A
Per2::Luc
Per2::Luc x GLP-1R-/-
Δ Phase (h)
6
0
-6
-12
##
##
= against PBS
PBS
OXM
PBS
OXM
B
Δ Phase (h)
6
0
-6
-12
#
*
###
***
= against solvent
PBS
NaOH
DMSO
GRI-2
GCG
GCG+GRI-2
OXM
OXM+GRI-2
C
CRE
500 bp
% of input
4
3
2
1
0
***
0'
OXM 30'
PBS 30'
0'
OXM 30'
PBS 30'

OXM Figure 2

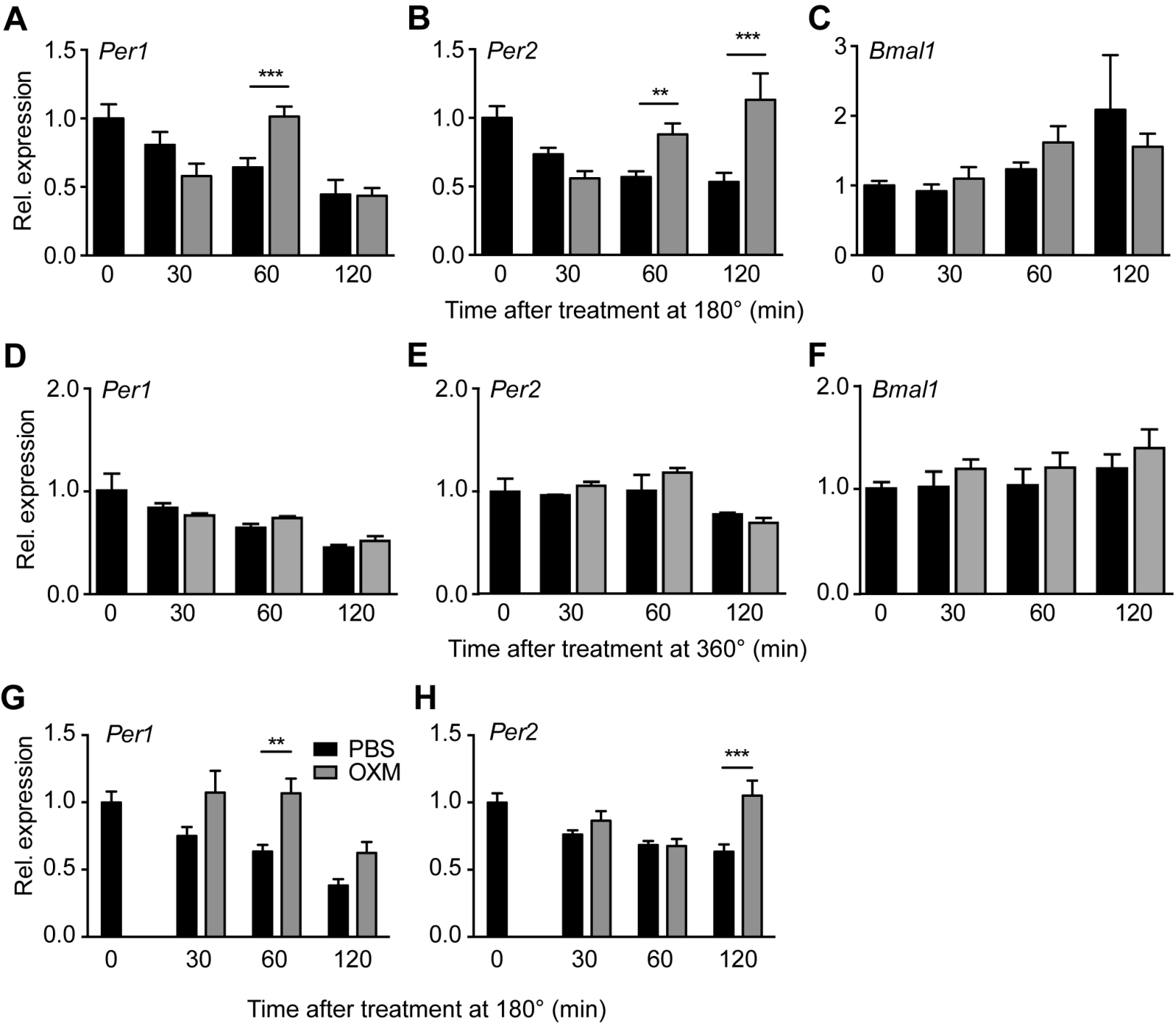
A
Per1
Rel. expression
1.5
1.0
0.5
0.0
***
0
30
60
120
B
Per2
***
**
C
Bmal1
3
2
1
0
Time after treatment at 180° (min)
D
Per1
2.0
E
Per2
F
Bmal1
Time after treatment at 360° (min)
G
Per1
PBS
OXM
H
Per2
Time after treatment at 180° (min)

OXM Figure 3

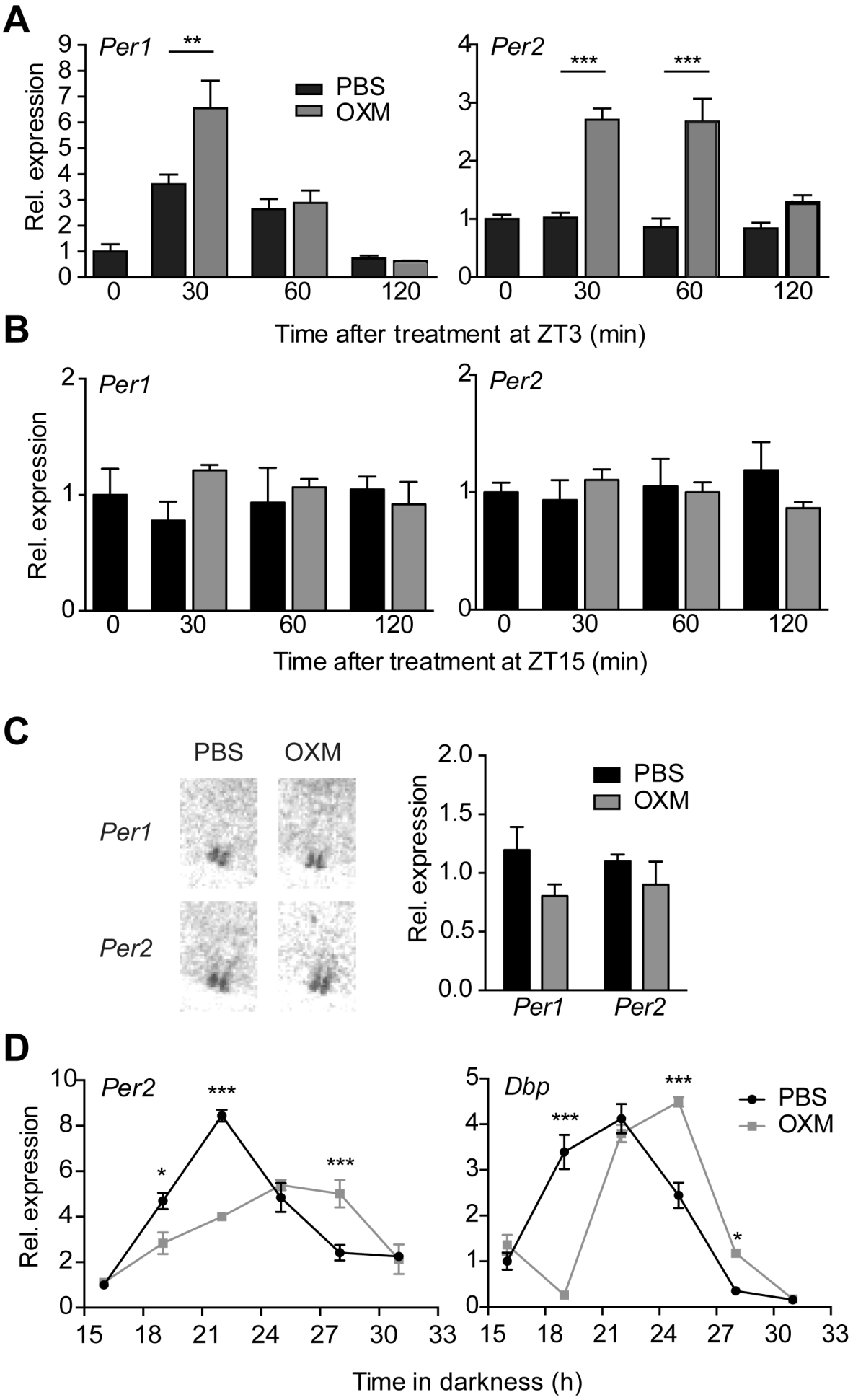
A
Per1
**
PBS
OXM
Rel. expression
Per2
***
***
0
30
60
120
Time after treatment at ZT3 (min)
B
Per1
Per2
Rel. expression
Time after treatment at ZT15 (min)
C
PBS
OXM
Per1
Per2
Rel. expression
Per1
Per2
D
Per2
Dbp
Rel. expression
Time in darkness (h)

OXM Figure 4

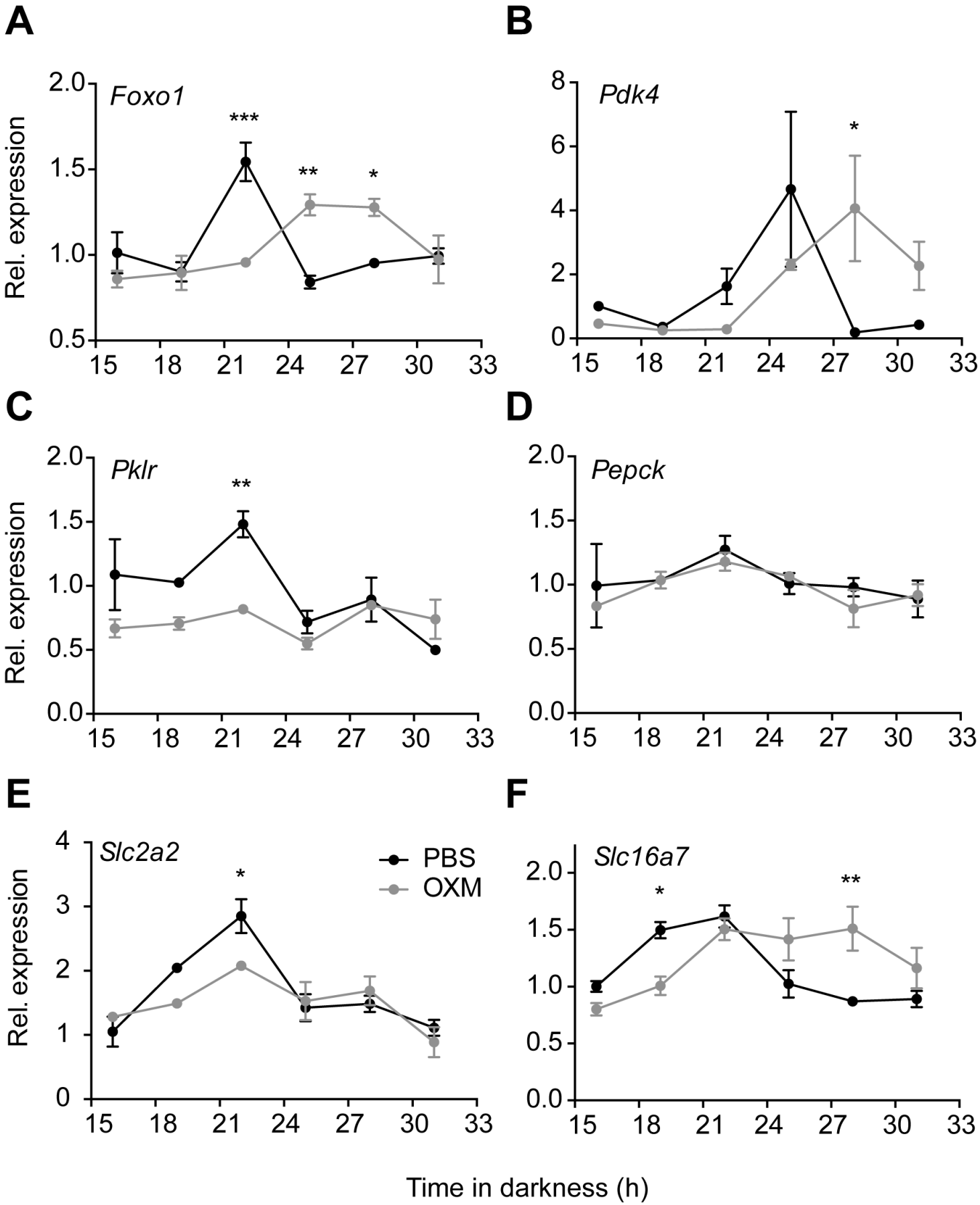
A
Foxo1
Rel. expression
2.0
1.5
1.0
0.5
***
**
*
15 18 21 24 27 30 33
B
Pdk4
8
6
4
2
0
*
15 18 21 24 27 30 33
C
Pklr
Rel. expression
2.0
1.5
1.0
0.5
0.0
**
15 18 21 24 27 30 33
D
Pepck
2.0
1.5
1.0
0.5
0.0
15 18 21 24 27 30 33
E
Slc2a2
Rel. expression
4
3
2
1
0
*
PBS
OXM
15 18 21 24 27 30 33
F
Slc16a7
2.0
1.5
1.0
0.5
0.0
*
**
15 18 21 24 27 30 33
Time in darkness (h)

OXM Figure 5

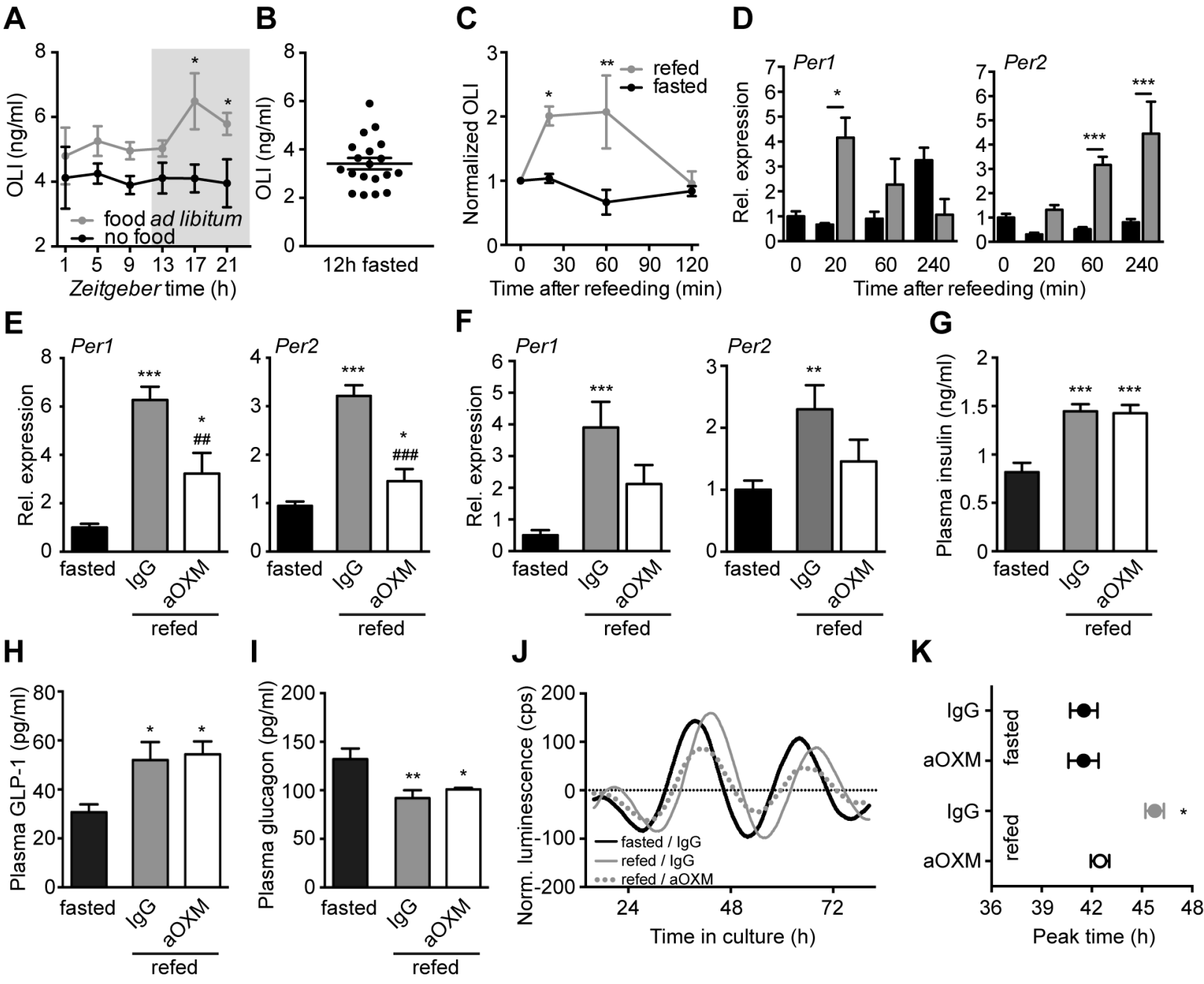
A
OLI (ng/ml)
food ad libitum
no food
Zeitgeber time (h)
B
OLI (ng/ml)
12h fasted
C
Normalized OLI
refed
fasted
Time after refeeding (min)
D
Per1
Per2
Rel. expression
Time after refeeding (min)
E
Per1
Per2
Rel. expression
fasted
IgG
aOXM
refed
F
Per1
Per2
Rel. expression
fasted
IgG
aOXM
refed
G
Plasma insulin (ng/ml)
fasted
IgG
aOXM
refed
H
Plasma GLP-1 (pg/ml)
fasted
IgG
aOXM
refed
I
Plasma glucagon (pg/ml)
fasted
IgG
aOXM
refed
J
Norm. luminescence (cps)
fasted / IgG
refed / IgG
refed / aOXM
Time in culture (h)
K
IgG
aOXM
fasted
IgG
aOXM
refed
Peak time (h)

OXM Figure 6